



**Railway deformation  
due to active  
sinkholes detected  
by DInSAR**

J. P. Galve et al.

This discussion paper is/has been under review for the journal Natural Hazards and Earth System Sciences (NHESS). Please refer to the corresponding final paper in NHESS if available.

# Railway deformation detected by DInSAR over active sinkholes in the Ebro Valley evaporite karst, Spain

J. P. Galve<sup>1</sup>, C. Castañeda<sup>2</sup>, and F. Gutiérrez<sup>3</sup>

<sup>1</sup>Departamento de Geodinámica, Universidad de Granada, Campus de Fuentenueva s/n, 18071 Granada, Spain

<sup>2</sup>Estación Experimental de Aula Dei, EEAD-CSIC, Ave. Montañana 1005, 50059 Zaragoza, Spain

<sup>3</sup>Departamento de Ciencias de la Tierra, Universidad de Zaragoza, C/Pedro Cerbuna 12, 50009 Zaragoza, Spain

Received: 25 May 2015 – Accepted: 28 May 2015 – Published: 16 June 2015

Correspondence to: J. P. Galve (jpgalve@ugr.es)

Published by Copernicus Publications on behalf of the European Geosciences Union.

Title Page

Abstract

Introduction

Conclusions

References

Tables

Figures



Back

Close

Full Screen / Esc

Printer-friendly Version

Interactive Discussion





5 areas affected by ground instability phenomena (Ge et al., 2008, 2013; Shi et al., 2010; Tan et al., 2010; Wu et al., 2010; Zhang et al., 2010; Chen et al., 2012; Hung et al., 2010). The instability processes that produce most problems in Chinese railways and are the main target of InSAR analyses are related to groundwater abstraction (Hung et al., 2010; Zhang et al., 2010) and permafrost (Chen et al., 2013; Shi et al., 2014). In a railway built upon permafrost, Shi et al. (2014) documented temporal variations of deformation in relation with rainfall and air temperature and measured higher strain in topographically lower areas, where water accumulation increases the impact of thawing and freezing.

10 Here, we present DInSAR displacement maps that reveal previously undetected active subsidence on sections of different railways in the surroundings of Zaragoza city, Ebro Valley evaporite karst, NE Spain (Fig. 1). One of the analysed areas includes two parallel railways, a conventional one and the Madrid–Barcelona high-speed line. Here, 1850 and 1900 m long sections are built on embankments and in excavated  
15 trenches, respectively. The latter are flanked by cuttings that expose subsidence structures. The other area with active subsidence includes a 4000 m long section of the conventional Castejón–Zaragoza railway (Fig. 1). Both railway corridors traverse large sinkholes previously documented in geomorphological maps (Simón et al., 1998, 2003; Galve et al., 2009). On 1 March 2003, a collapse sinkhole 5 m across formed beneath  
20 the high-speed railway a few months before its inauguration (Guerrero et al., 2008). We observed obvious deformation in a poorly maintained subsidiary railroad of the Castejón–Zaragoza line, coinciding with the location of an active sinkhole mapped on the basis of geomorphic criteria (Fig. 2). Moreover, on 11 September 1991, a collapse sinkhole caused the derailment of a freight train in the conventional Madrid–Barcelona railway downstream of Zaragoza city (at km 360.7; Gutiérrez et al., 2007). In this work  
25 we integrate DInSAR deformation data with different subsidence evidence (geomorphic, deformed sediments, damaged human structures). The convergence of the different lines of evidence is used to support the utility of DInSAR for monitoring railways affected by dissolution-induced subsidence.

---

## Railway deformation due to active sinkholes detected by DInSAR

J. P. Galve et al.

---

[Title Page](#)[Abstract](#)[Introduction](#)[Conclusions](#)[References](#)[Tables](#)[Figures](#)[Back](#)[Close](#)[Full Screen / Esc](#)[Printer-friendly Version](#)[Interactive Discussion](#)

## 2 SAR data and processing methods

Archived data from two orbital SAR missions have been used to produce the InSAR deformation maps analysed in this work. One of the datasets includes C-band data of 29 ENVISAT ASAR images acquired at 10:00 p.m. on ascending orbits from 2 May 2003 to 17 September 2010 (track 58, frame 829). The other dataset comprises L-band data of 13 ALOS PALSAR images acquired at 10:30 p.m. on ascending mode, HH polarisation, and covering a period from 12 February 2007 to 7 April 2010 (track 665, frame 820).

The SAR images were processed using the Stable Point Network (SPN) technique (Crosetto et al., 2008). Pre-processing was carried out using the DIAPASON interferometric algorithm (Massonet and Feigl, 1998). This algorithm incorporates the persistent scatterers and the distributed scatterers approaches based on full resolution and medium resolution data, respectively. The topographic component of the interferometric phase was removed using the Spanish photogrammetric elevation model “GISOleícola” with a spatial resolution of 20 m.

The ENVISAT-ASAR-derived displacement rate map was produced at full resolution from a total of 61 interferograms. The persistent scatterers (PS) were selected establishing a coherence threshold of 0.46 on the basis of the SAR amplitude selection criterion. The average LOS displacement rate and the LOS displacement time series of each PS were derived from the Single Look Complex (SLC) ASAR images. Current Displacement rate values  $> 2 \text{ mm yr}^{-1}$  were considered as non-stable points. The ALOS-PALSAR-derived displacement rate map was produced at a ground resolution of about  $25 \text{ m} \times 25 \text{ m}$  and establishing a coherence threshold of 0.40. In this case, displacement rates  $> 4 \text{ mm yr}^{-1}$  were considered as indicative of surface deformation.

**NHESSD**

3, 3967–3981, 2015

### **Railway deformation due to active sinkholes detected by DInSAR**

J. P. Galve et al.

Title Page

Abstract

Introduction

Conclusions

References

Tables

Figures

◀

▶

◀

▶

Back

Close

Full Screen / Esc

Printer-friendly Version

Interactive Discussion



### 3 Railway deformation detected by DInSAR and interpretation

Railways behaved as good reflection features for ALOS and ENVISAT sensors, providing a relatively high density of measurement points, especially in the ALOS-derived map. Two profiles of LOS displacement rates have been constructed along the Castejón–Zaragoza and Madrid–Zaragoza corridors using the ALOS and ENVISAT maps, respectively (Fig. 3).

The displacement rates measured in the SW and NE portions of the analyzed Madrid–Zaragoza railway section, as high as  $-6.6 \text{ mm yr}^{-1}$ , may be related to compaction of the embankments, as suggest the direct correlation between subsidence rates and embankment height (Fig. 3, Profile 1). LOS displacement rates indicate rapid settlement ( $> 4 \text{ mm yr}^{-1}$ ) in the NE sector of the analysed stretch, coinciding with the location of a buried depression of unknown origin, filled a few decades ago and identified with aerial photographs. Here, subsidence is most probably related to compaction of anthropogenic deposits, which may exceed 10 m including the embankment. However, further investigations would be required to rule out the potential contribution of dissolution-induced subsidence (e.g. trenching, geophysics, vertical extensometers).

The negative LOS displacement values measured in the sector where the right-of-way of the railway has been excavated in Quaternary alluvium can be attributed to dissolution-induced subsidence. Between 1500 and 2700 m in profile 1, there is a significant number of points with LOS displacement rates below  $-2 \text{ mm yr}^{-1}$ . In this sector, the railways run across subdued sinkholes recognized in old aerial photographs and expressed in the cuttings as deformed Quaternary alluvium (Simón et al., 1998, 2003; Galve et al., 2009). The sinkhole cluster comprises a large diffuse-edged depression and several smaller subcircular sinkholes (Galve et al., 2009) (Fig. 4). In addition to the DInSAR deformation data, several lines of evidence consistently indicate active subsidence in some sectors of the sinkhole cluster: enclosed depressions, severe cracking on buildings, conspicuous sags and wide fissures on roads and small collapse sinkholes, including the 2003 event. An excavation carried out at the SW edge of the large

**NHESSD**

3, 3967–3981, 2015

#### **Railway deformation due to active sinkholes detected by DInSAR**

J. P. Galve et al.

Title Page

Abstract

Introduction

Conclusions

References

Tables

Figures

◀

▶

◀

▶

Back

Close

Full Screen / Esc

Printer-friendly Version

Interactive Discussion



depression for the foundation of a bridge exposed tilted Quaternary deposits dipping toward the depression center (Fig. 4). Two sedimentary packages were differentiated. The lower one corresponds to pre-sinkhole terrace gravel deposits with an apparent NE dip of 14–17°. The upper one is a natural sinkhole fill deposits that pinches out towards the SW (sinkhole edge). The dip of these sediments progressively attenuates upwards (cumulative wedge-out) suggesting synsedimentary subsidence.

The high density of measurement points derived from the ALOS data along the Castejón–Zaragoza railway provides valuable information on the state of activity of three previously inventoried sinkholes traversed by the infrastructure. A clear subsidence zone, with negative LOS displacement rates as high as  $-9.7 \text{ mm yr}^{-1}$ , coincides with a sinkhole about 300 m across previously classified as active (Figs. 2 and 3, Profile 2). Here, ground motion values show a consistent pattern with increasing subsidence rates towards the center of the sinkhole (Fig. 2). The LOS displacement values measured in the other two sinkholes, previously described as inactive (Galve et al., 2009), suggest ground stability or very slow subsidence ( $< 2 \text{ mm yr}^{-1}$ ).

## 4 Discussion

The presented data illustrates that DInSAR offers a promising potential for monitoring railways affected by sinkhole activity and dissolution-induced subsidence. This postulate is supported by two relevant aspects of our investigation: (1) there is a good spatial correlation between the deformation values measured by DInSAR and unambiguous field evidence of active subsidence associated with sinkholes. (2) DInSAR analyses focused on the railway tracks or specific sections of the infrastructure would provide better results than the deformation values presented in this work, derived from a regional investigation with a limited spatial resolution (Galve et al., 2015).

Railways are linear features commonly laying on relatively flat surfaces that behave as adequate reflectors for the spaceborne SAR systems, providing spatially dense and temporarily stable coherent scatterers (Hanssen et al., 2009; Shi et al., 2014). Chen

## Railway deformation due to active sinkholes detected by DInSAR

J. P. Galve et al.

Title Page

Abstract

Introduction

Conclusions

References

Tables

Figures

◀

▶

◀

▶

Back

Close

Full Screen / Esc

Printer-friendly Version

Interactive Discussion



**Railway deformation due to active sinkholes detected by DInSAR**

J. P. Galve et al.

Title Page

Abstract

Introduction

Conclusions

References

Tables

Figures



Back

Close

Full Screen / Esc

Printer-friendly Version

Interactive Discussion



et al. (2012) illustrates the strong backscattering of railways in ALOS PALSAR and ENVISAT ASAR amplitude images, compared with the surrounding features. The density of natural reflection points on the railway track depends on their relative orientation with respect to the flight path of the sensor. However, in our case, both the ENVISAT and ALOS data correspond to ascending paths and, consequently, the differences observed between the two DInSAR displacement rate maps cannot be attributed to the course of the satellites. Ge et al. (2008) and Shi et al. (2010) have obtained deformation sequences covering long time spans analyzing PSs along railways. Shi et al. (2010) measured numerous minor and locally distributed displacements that were not detected by leveling. Chen et al. (2012) obtained a higher density of PSs with ALOS PALSAR data than with ENVISAT ASAR data. This was probably due to the higher critical baseline and the longer wavelength of the former, resulting in higher coherence, especially in zones with high deformation gradients and in man-made features such as the railway embankment. This author inferred that the difference in the distribution of PSs derived from L-band and C-band data are controlled by their different scattering mechanism. In PALSAR results, the railway embankment was more easily detected because of its resolution (10 m). Man-made linear features were dominated by the dihedral scattering and resulted in high density of PS points in PALSAR results. For ENVISAT data, despite the strong backscattering of the railway, motion may not be recorded using PS method due to the multiple scattering of the different surfaces.

PS detection in linear infrastructures is improving substantially by using high resolution data (e.g. CosmoSkyMed, TerraSAR-X) (Ge et al., 2013; Nutricato et al., 2013; Yu et al., 2013; Luo et al., 2014). Yu et al. (2013) found dense PSs in highways and railways using high resolution TerraSAR-X data due to the presence of numerous stable objects distributed along the infrastructures, like lamps, stones or fences.

## 5 Conclusions and final considerations

DInSAR techniques helped in the detection of previously unknown actual settlement that slightly deforms several stretches of two principal railway lines of NE Spain in the outskirts of Zaragoza city; a region affected by evaporite karst subsidence. The recognition of this deformation has been possible thanks to high resolution surface velocity maps generated through the analysis of archived data of the ENVISAT and ALOS SAR missions. The results show that DInSAR methods allows to identify and monitor deformation on railways that may compromise the comfort and safety of travellers. This particularly applies for railways lines that go through areas with problematic ground conditions.

DInSAR velocity maps coupled with detailed geomorphological maps may help in the identification and characterization of the railway stretches liable to be intensively monitored. This stretches may be controlled by using real-time advanced ground-based monitoring techniques such as motorized total station systems that measure prisms attached directly to the structure or time-domain reflectometry (TDR) coaxial cable sensors. DInSAR also could be an alternative to these expensive techniques where the ground deformation does not result in a medium-high risk situation. Site-specific investigations combining more adequate and higher resolution SAR data with ground references (e.g. corner reflectors, GPS benchmarks) may provide a very precise monitoring system. Future studies should focus on the deformation monitoring using TerraSAR-X, COSMO-SkyMed data coupled with other ground-based measurements.

*Acknowledgements.* This research has been funded by the Spanish national projects CGL2010-16775, AGL2012-40100 and CGL2013-40867-P (Spanish Ministry of Economy and Competitiveness and FEDER), the Regional projects 2012/GA-LC-021 and 2012/GA LC 036 (DGA-La Caixa) and the European Interreg IV B SUDOE project DO-SMS-SOE1/P2/F157. Jorge Pedro Galve has been contracted under the DGA-La Caixa project. SPN maps (derived from ENVISAT and ALOS data) were produced by Altamira Information S.L. (Spain). The 2009 orthoimages are products of the National Geographic Institute of Spain (Instituto Geográfico Nacional) available at: <http://centrodedescargas.cnig.es/CentroDescargas/index.jsp>.

### Railway deformation due to active sinkholes detected by DInSAR

J. P. Galve et al.

Title Page

Abstract

Introduction

Conclusions

References

Tables

Figures



Back

Close

Full Screen / Esc

Printer-friendly Version

Interactive Discussion





## References

- Chen, F., Lin, H., Li, Z., Chen, Q., and Zhou, J.: Interaction between permafrost and infrastructure along the Qinghai–Tibet Railway detected via jointly analysis of C- and L-band small baseline SAR interferometry, *Remote Sens. Environ.*, 123, 532–540, doi:10.1016/j.rse.2012.04.020, 2012. 3969, 3972, 3973
- Chen, F., Lin, H., Zhou, W., Hong, T., and Wang, G.: Surface deformation detected by ALOS PALSAR small baseline SAR interferometry over permafrost environment of Beiluhe section, Tibet Plateau, China, *Remote Sens. Environ.*, 138, 10–18, doi:10.1016/j.rse.2013.07.006, 2013. 3969
- Crosetto, M., Biescas, E., Duro, J., Closa, J., and Arnaud, A.: Generation of advanced ERS and Envisat interferometric SAR products using the stable point network technique, *Photogramm. Eng. Rem. S.*, 74, 443–450, 2008. 3970
- Galve, J. P., Gutiérrez, F., Lucha, P., Bonachea, J., Remondo, J., Cendrero, A., Gutiérrez, M., Gimeno, M. J., Pardo, G., and Sánchez, J. A.: Sinkholes in the salt-bearing evaporite karst of the Ebro River valley upstream of Zaragoza city (NE Spain), *Geomorphology*, 108, 145–158, doi:10.1016/j.geomorph.2008.12.018, 2009. 3969, 3971, 3972
- Galve, J. P., Castañeda, C., Gutiérrez, F., and Herrera, G.: Assessing sinkhole activity in the Ebro Valley mantled evaporite karst using advanced DInSAR, *Geomorphology*, 229, 30–44, 2015. 3972
- Ge, D., Wang, Y., Guo, X., Wang, Y., and Xia, Y.: Land subsidence investigation along railway using permanent scatterers SAR interferometry, in: *Geosci. Remote Sens. Symp. 2008, IGARSS 2008, IEEE Int.*, 2, II–1235–II–1238, doi:10.1109/IGARSS.2008.4779225, Boston, Massachusetts, USA, 6–11 July 2008. 3969, 3973
- Ge, D., Wang, Y., Zhang, L., Xia, Y., Wang, Y., and Guo, X.: Using permanent scatterer InSAR to monitor land subsidence along High Speed Railway-the first experiment in China. *Proceedings of “Fringe 2009 Workshop”, Frascati, Italy, 30 November–4 December 2009.*
- Ge, D., Wang, Y., Zhang, L., Li, M., and Guo, X.: Integrating medium and high resolution PSInSAR data to monitor terrain motion along large scale manmade linear features – a case study in Shanghai, in: *Geosci. Remote Sens. Symp. (IGARSS), 2013 IEEE Int.*, 4034–4037, doi:10.1109/IGARSS.2013.6723718, Melbourne, Australia, 21–26 July 2013. 3969, 3973
- Gourc, J. P., Villard, P., Giraud, H.: Full scale experimentation of discontinuous subsidence for railway and motorway embankments, in: *Proceedings of the Twelfth European Conference on*

## NHESSD

3, 3967–3981, 2015

### Railway deformation due to active sinkholes detected by DInSAR

J. P. Galve et al.

Title Page

Abstract

Introduction

Conclusions

References

Tables

Figures



Back

Close

Full Screen / Esc

Printer-friendly Version

Interactive Discussion



## Railway deformation due to active sinkholes detected by DInSAR

J. P. Galve et al.

Title Page

Abstract

Introduction

Conclusions

References

Tables

Figures



Back

Close

Full Screen / Esc

Printer-friendly Version

Interactive Discussion



Soil Mechanics and Geotechnical Engineering; Geotechnical Engineering for Transportation Infrastructure; Theory and Practice, Planning and Design, Construction and Maintenance, edited by: Barends, F. B. J., Lindenberg, J., Luger, H. J., Quelerij, L., and Verruijt, A., A. A. Balkema, Rotterdam, 1789–1794, Amsterdam, Netherlands, 7–10 June 1999 3968

5 Guerrero, J., Gutiérrez, F., Bonachea, J., and Lucha, P.: A sinkhole susceptibility zonation based on paleokarst analysis along a stretch of the Madrid–Barcelona high-speed railway built over gypsum- and salt-bearing evaporites (NE Spain), *Eng. Geol.*, 102, 62–73, 2008. 3968, 3969

10 Gutiérrez, F., Galve, J. P., Guerrero, J., Lucha, P., Cendrero, A., Remondo, J., Bonachea, J., Gutiérrez, M., and Sánchez, J. A.: The origin, typology, spatial distribution and detrimental effects of the sinkholes developed in the alluvial evaporite karst of the Ebro River valley downstream of Zaragoza city (NE Spain), *Earth Surf. Proc. Land.*, 32, 912–928, 2007. 3969

Hanssen, R. F. and van Leijen, F. J.: One-dimensional radar interferometry for line infrastructure, in: *Geosci. Remote Sens. Symp. IEEE Int. 2009*, 5, V–9–V–12, doi:10.1109/IGARSS.2009.5417745, ape Town, South Africa, 12–17 July 2009. 3972

15 Hung, W.-C., Hwang, C., Chang, C.-P., Yen, J.-Y., Liu, C.-H., and Yang, W.-H.: Monitoring severe aquifer-system compaction and land subsidence in Taiwan using multiple sensors: Yunlin, the southern Choushui River Alluvial Fan, *Environ. Earth Sci.*, 59, 1535–1548, doi:10.1007/s12665-009-0139-9, 2010. 3969

20 Luo, Q., Perissin, D., Lin, H., Zhang, Y., and Wang, W.: Subsidence monitoring of Tianjin suburbs by TerraSAR-X persistent scatterers interferometry, *IEEE J. Sel. Top. Appl.*, 7, 1642–1650, doi:10.1109/JSTARS.2013.2271501, 2014. 3973

Massonnet, D. and Feigl, K. L.: Radar interferometry and its application to changes in the Earth's surface, *Rev. Geophys.*, 36, 441–500, doi:10.1029/97RG03139, 1998. 3970

25 Nutricato, R., Nitti, D. O., Bovenga, F., Refice, A., Wasowski, J., and Chiaradia, M. T.: C/X-band SAR interferometry applied to ground monitoring: examples and new potential, in: *Proc. of SPIE*, 88910C-1, 88910C–88910C–9, doi:10.1117/12.2029096, 2013. 3973

Shi, H., Yang, S., Wei, Q., and Tan, Q.: Study on the establishment of integrated HSR subsidence monitoring system based on InSAR technique, in: *International Conference on Railway Engineering, ICRE2010 Proceedings*, 729–734, Beijing, China, 20–21 August 2010. 3969, 3973

30 Shi, X., Liao, M., Wang, T., Zhang, L., Shan, W., and Wang, C.: Expressway deformation mapping using high-resolution TerraSAR-X images, *Remote Sens. Lett.*, 5, 194–203, doi:10.1080/2150704X.2014.891774, 2014. 3969, 3972

## Railway deformation due to active sinkholes detected by DInSAR

J. P. Galve et al.

Title Page

Abstract

Introduction

Conclusions

References

Tables

Figures

◀

▶

◀

▶

Back

Close

Full Screen / Esc

Printer-friendly Version

Interactive Discussion



Simón, J., Soriano, M., Arlegui, L., Casas, A., Liesa, C., Pocoví, A., Gracia, J., and Salvador, T.: Evaluación del riesgo de hundimientos por dolinas en el trazado de las nuevas estructuras ferroviarias en el entorno de Zaragoza (informe complementario), available at: <http://estaticos.elmundo.es/documentos/2003/10/03/informeave.doc> (last access: 20 May 2015), 2003. 3969, 3971

Simón, J. L., Soriano, M. A., Arlegui, L., and Caballero, J.: Estudio de riesgos de hundimientos kársticos en el corredor de la Carretera de Logroño, available at: <http://www.zaragoza.es/contenidos/urbanismo/pgouz/memoria/anejos/anejo03/anejo032.pdf> (last access: 20 May 2015), 1998. 3969, 3971

Tan, Q., Xie, C., and Yang, S.: A new surveying technology for railway subgrade settlement deformation monitoring: a case study, in: ICRE2010 – International Conference on Railway Engineering Proceedings, 404–407, Beijing, China, 20–21 August 2010. 3969

Wu, H., Zhang, Y., Zhang, J., and Chen, X.: Mapping deformation of man-made linear features using DInSAR technique, in: ISPRS TC VII Symposium – 100 Years ISPRS – IAPRS, Vol. XXXVIII, Part 7A, edited by: Wagner, W. and Székely, B., Vienna, Austria, 293–297, Vienna, Austria, 5–7 July 2010. 3969

Xuedong, Z., Daqing, G., Weiyu, M., Ling, Z., Dapeng, Y., and Xiaofang, G.: Study the land subsidence along JingHu highway (Beijing–Hebei) using PS-InSAR technique, in: Geosci. Remote Sens. Symp. (IGARSS), 2011 IEEE Int., 1608–1611, doi:10.1109/IGARSS.2011.6049538, Vancouver, Canada, 24–29 July 2011.

Yu, B., Liu, G., Zhang, R., Jia, H., Li, T., Wang, X., Dai, K., and Ma, D.: Monitoring subsidence rates along road network by persistent scatterer SAR interferometry with high-resolution TerraSAR-X imagery, *J. Modern Transportation*, 21, 236–246, doi:10.1007/s40534-013-0030-y, 2013. 3973

Zhang, H., Tao, L., Wang, C., and Tang, Y.: Ground deformation detection along Beijing–Tianjin intercity railway using advanced network multi-baseline DInSAR, in: Wavelet Anal. Pattern Recognit. (ICWAPR), 2010 Int. Conf., 222–226, doi:10.1109/ICWAPR.2010.5576333, Qingdao, China, 11–14 July, 2010. 3969

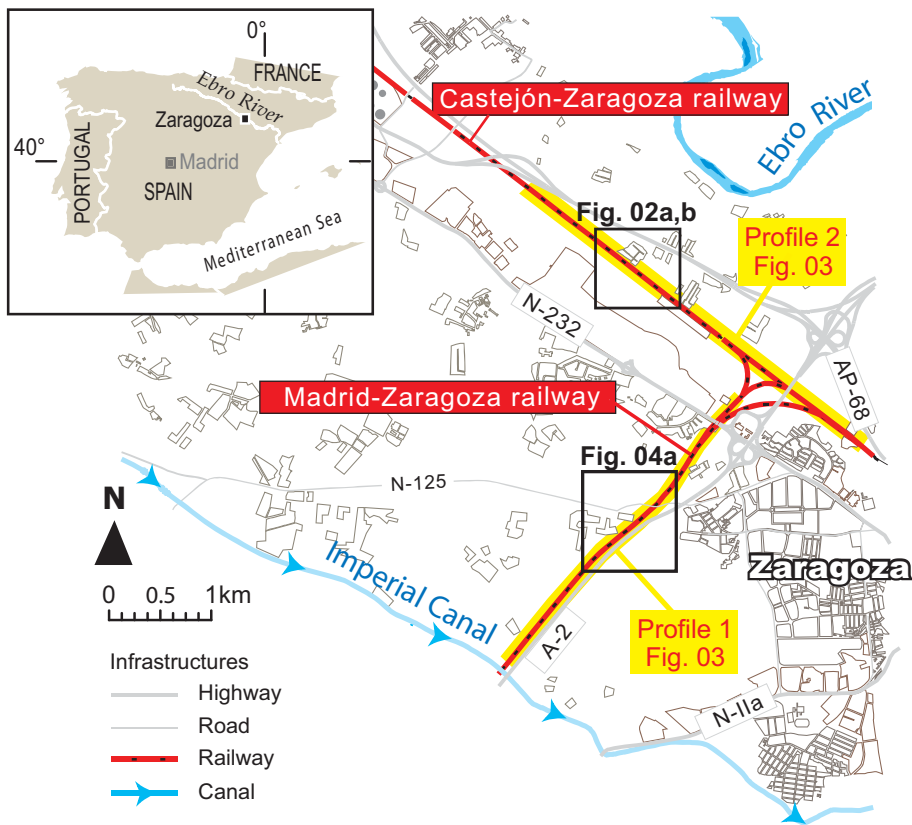


**Figure 1.** Geographic location of the studied railway sections.

**Railway deformation due to active sinkholes detected by DInSAR**

J. P. Galve et al.

Title Page	
Abstract	Introduction
Conclusions	References
Tables	Figures
◀	▶
◀	▶
Back	Close
Full Screen / Esc	
Printer-friendly Version	
Interactive Discussion	



## Railway deformation due to active sinkholes detected by DInSAR

J. P. Galve et al.

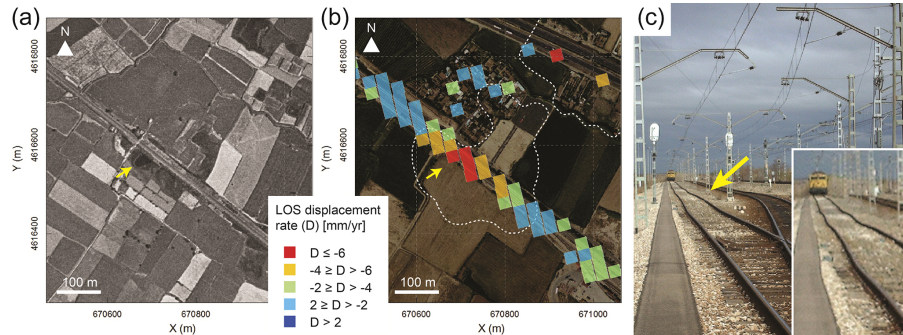


**Figure 2.** Section of the Castejón–Zaragoza railway built on a buried sinkhole and affected by active karst subsidence. **(a)** Aerial photograph taken in 1956. Arrow points to a ponded sector within the large subsidence depression. **(b)** Orthoimage from 2009 with ALOS-derived displacement rates on PSs. **(c)** Photographs of the location indicated with arrows in **(a)** and **(b)**, showing obvious deformation in the railways.

Title Page

Abstract

Introduction

Conclusions

References

Tables

Figures

◀

▶

◀

▶

Back

Close

Full Screen / Esc

Printer-friendly Version

Interactive Discussion



## Railway deformation due to active sinkholes detected by DInSAR

J. P. Galve et al.

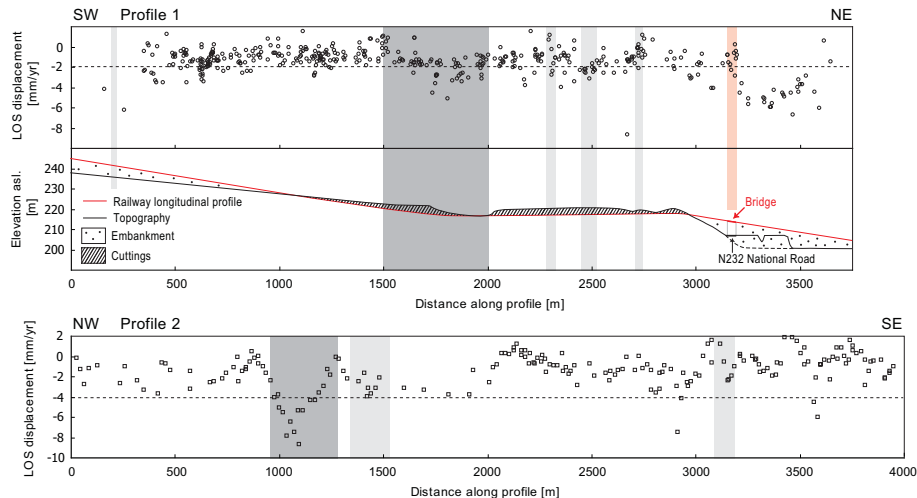


**Figure 3.** Profiles with DInSAR-derived LOS deformation data obtained along the analyzed railway sections. Data from the Madrid–Barcelona railway corridor is represented alongside a topographic profile showing the stretches built on embankment and excavated trenches. Dark grey and light grey zones indicate sections built on sinkholes classified as active and inactive, respectively. See location of profiles in Fig. 1.

[Title Page](#)
[Abstract](#)
[Introduction](#)
[Conclusions](#)
[References](#)
[Tables](#)
[Figures](#)
[◀](#)
[▶](#)
[◀](#)
[▶](#)
[Back](#)
[Close](#)
[Full Screen / Esc](#)
[Printer-friendly Version](#)
[Interactive Discussion](#)


## Railway deformation due to active sinkholes detected by DInSAR

J. P. Galve et al.

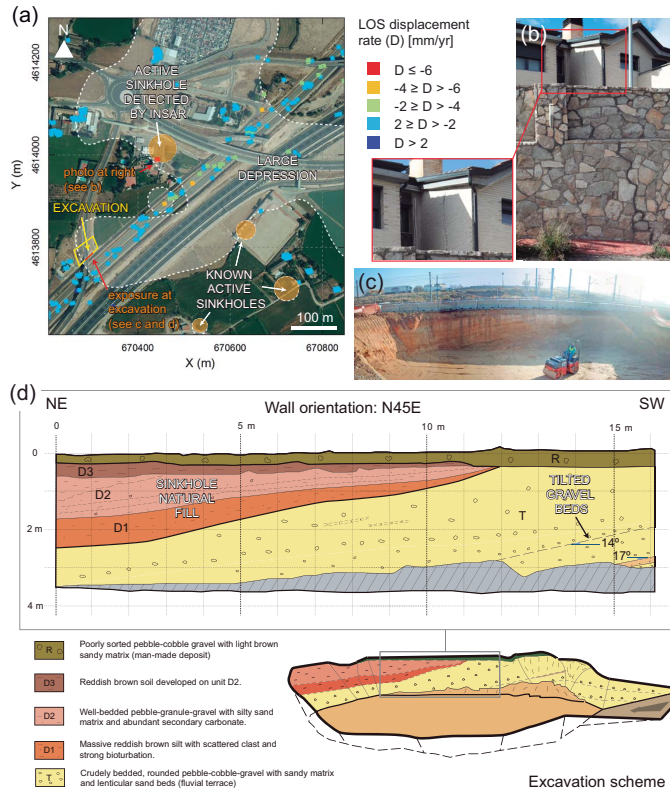


**Figure 4.** Evidence of karst subsidence associated with the track of the Madrid–Zaragoza high-speed railway. **(a)** Orthoimage of 2009 with ENVISAT DInSAR PS data indicating the main sinkholes and large karst depressions. **(b)** Cracks on a house where ENVISAT DInSAR map indicate subsidence. **(c)** General view of the excavation indicated in **(a)**. **(d)** Log and scheme of the walls of the excavation. Note the wedging-out of the sinkhole fill and the tilted terrace gravel beds.

[Title Page](#)
[Abstract](#)
[Introduction](#)
[Conclusions](#)
[References](#)
[Tables](#)
[Figures](#)
[Back](#)
[Close](#)
[Full Screen / Esc](#)
[Printer-friendly Version](#)
[Interactive Discussion](#)